2,4,6-Triarylchalcogenopyrylium Dyes Related in Structure to the Antitumor Agent AA1 as in Vitro Sensitizers for the Photodynamic Therapy of Cancer

Kristi A. Leonard,[†] Marina I. Nelen,[†] Linda T. Anderson,[‡] Scott L. Gibson,[‡] Russell Hilf,[‡] and Michael R. Detty*[,†]

Departments of Chemistry and Medicinal Chemistry, State University of New York at Buffalo, Buffalo, New York 14260, and Department of Biochemistry and Biophysics, University of Rochester Medical Center, 601 Elmwood Avenue, Box 607, Rochester, New York 14642

Received March 22, 1999

Cationic chalcogenopyrylium dyes **2**−**4** were synthesized in six steps from 4-(dimethylamino)-phenylethyne (**7**), have absorption maxima in methanol of 594, 631, and 672 nm, respectively, and generate singlet oxygen with quantum yields [$\Phi(^1O_2)$] of 0.020, 0.064, and 0.037, respectively. Dyes **2**−**4** are hydrolytically more stable than other chalcogenopyrylium dyes evaluated previously as sensitizers for photodynamic therapy. At 10 μM final concentration, all dyes **2**−**4** inhibited cytochrome *c* oxidase during irradiation of tumor mitochondrial suspensions treated with 10 μM dye. The degree of enzyme inhibition was abated in a reduced oxygen environment and in the presence of imidazole, a singlet oxygen trap. Superoxide dismutase, at a final concentration of 30 U, did not alter the photosensitized inhibition of mitochondrial cytochrome *c* oxidase by dyes **2**−**4**. These data suggest that singlet oxygen may play a major role in the photosensitized inhibition of mitochondrial cytochrome *c* oxidase. Irradiation of R3230AC rat mammary adenocarcinoma cells in the presence of dyes **2**−**4** caused a significant loss in cell viability with thiopyrylium dye **2** displaying the greatest phototoxicity. Initial acute toxicity studies in vivo demonstrate that, at 10 mg/kg, none of the three dyes displayed overt toxicity.

Introduction

Photodynamic therapy (PDT) has been developed as a cancer therapy over the last 25 years and has regulatory approval in the United States, Canada, The Netherlands, France, Germany, and Japan for cancers of the lung, digestive tract, and genitourinary tract.[1] PDT has also been evaluated as a protocol for treating cancers of the head and neck region[2] and for treating pancreatic cancer.[3] As a therapy, PDT uses a light-activated sensitizer to produce a cytotoxic reagent or a cytotoxic reaction in the tumor cell, typically via generation of singlet oxygen or superoxide from molecular oxygen.[1a] Photofrin, a derivative of hematoporphyrin, has received regulatory approval for use in PDT, but Photofrin is not an ideal sensitizer and many other porphyrins and porphyrin-related molecules have been prepared and evaluated in the search for improved sensitizer properties.[4,5] Photofrin and other porphyrin derivatives have relatively weak absorption in the 700−900-nm spectral window where optimal penetration of light into tissue is afforded.[6] Many of these sensitizers also cause long-term skin photosensitivity in patients.[1]

Cationic sensitizers for PDT are complementary to Photofrin and related compounds in that cationic dyes appear to be bound intracellularly. Cationic sensitizers for PDT evolved from studies with rhodamine 123 (Rh-123; Chart 1), which is taken up by mitochondria in living cells and has been reported to accumulate to a greater extent in malignant cells relative to normal cells.[7] However, Rh-123 is relatively inefficient as a photosensitizer due to its poor quantum yield for singlet oxygen generation, even when immobilized in the lipophilic medium of the mitochondrial membrane. Heavy-atom analogues of Rh-123 have been prepared, and a tetrabromo derivative has been found to be more effective as a sensitizer than Rh-123 against certain cell

Chart 1

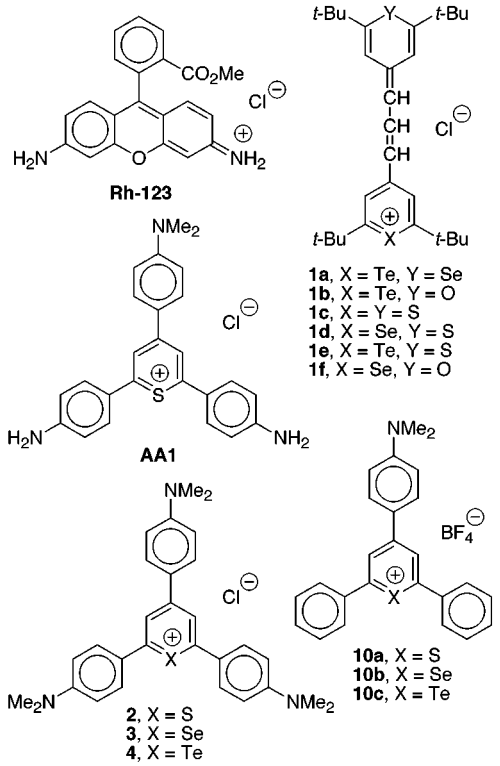

* To whom correspondence should be addressed.
[†] State University of New York at Buffalo.
[‡] University of Rochester Medical Center.

10.1021/jm990134r CCC: $18.00
Published on Web 09/03/1999

Scheme 1

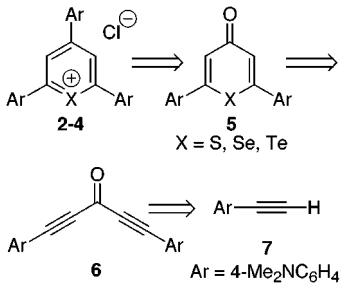

lines.[8] However, absorption of light by both Rh-123 and its heavy-atom analogues is of too short a wavelength for the deep tissue penetration desired for PDT.

Other cationic dyes absorbing at longer wavelengths have been explored as sensitizers for PDT including the Victoria blues,[9] methylene blues[10] and the related nile blues,[11] cyanine dyes,[12] rhodacyanine dyes,[13] and telluropyrylium dyes.[14] The cationic thiopyrylium dye AA1 (Chart 1) has been described as a mitochondrial-specific antitumor agent.[15] AA1 shares structural features with the rhodamines, Victoria blues, nile blues, and methylene blues. All of these cationic dyes have two amino groups separated by roughly 9−11 Å that are conjugated to the π-framework thus delocalizing the positive charge of the molecule. Although AA1 has a maximum of absorption of 550 nm, AA1 still weakly absorbs wavelengths of light longer than 600 nm. Despite its similarities to other cationic photosensitizers, AA1 shows no photosensitivity in cell culture.[15] We were interested in the design of AA1 analogues that might function as photosensitizers.

In our earlier studies with chalcogenopyrylium dyes **1** (Chart 1), we demonstrated that better sensitizers for PDT were obtained by substituting heavier chalcogen atoms (Se, Te) for lighter chalcogen atoms (O, S) in the dye chromophore.[14a] Substitution of the heavier chalcogen atoms results in dye chromophores with longer wavelengths of absorption and higher rates of intersystem crossing of the singlet excited state to the triplet state.[16] The latter process leads to higher quantum yields for singlet oxygen generation for dyes incorporating the heavier chalcogen atoms. We have applied this approach to the preparation of selenium- and tellurium-containing analogues of AA1-like molecules. The chalcogenopyrylium dyes **2**−**4** (Chart 1) bearing 4-(dimethylamino)phenyl substituents at 2-, 4-, and 6-positions represent a new class of dyes that function as in vitro sensitizers for PDT. All three dyes including the thiopyrylium dye **2** displayed in vitro phototoxicity against R3230AC mammary adenocarcinoma cells and inhibited cytochrome *c* oxidase activity upon irradiation of isolated mitochondria.

Chemistry

Retrosynthetic Analysis and Synthesis. While thiopyrylium and selenopyrylium dyes have been prepared via several different routes, telluropyrylium dyes have been prepared only from telluropyranone precursors.[17] This limitation dictated our synthetic approach to dyes **2**−**4**, whose retrosynthesis is outlined in Scheme 1. The chalcogenopyranones **5** serve as precursors to thio-, seleno-, and telluropyrylium dyes through the addition of nucleophilic reagents to the 4-position.[18,19] The addition of the Grignard reagent from 4-bromo-*N*,*N*-dimethylaniline to the carbonyl carbon of chalcogenopyranones **5**[18,19] followed by acid-induced dehydration represents a direct route to dyes **2**−**4**.[19] The chalcogenopyranones **5** can be prepared in turn via the formal addition of hydrogen sulfide, selenide, or telluride to 1,4-pentadiyn-3-one **6**, which serves as a common precursor to dyes **2**−**4**.[18] The symmetrical diynone **6** can be prepared from the equivalent of coupling two molecules of 4-(dimethylamino)phenylacetylene (**7**)[20] with methyl formate.

Acetylene **7** was prepared in 74% overall yield by the palladium-catalyzed coupling of trimethylsilylacetylene and 4-bromo-*N*,*N*-dimethylaniline to give trimethylsilyl-4-(dimethylamino)phenylacetylene, which was then desilylated with tetrabutylammonium fluoride (Scheme 2).[20] *n*-Butyllithium was added to **7** to generate the corresponding lithium acetylide, which then was added to methyl formate to give 1,5-di-4-(dimethylamino)-phenyl-1,4-pentadiyn-3-ol (**8**) in 57% isolated yield. Diynol **8** was oxidized to 1,5-di-4-(dimethylamino)-phenyl-1,4-pentadiyn-3-one (**6**) in 81% isolated yield with manganese dioxide in dichloromethane.

The formal addition of hydrogen chalcogenides to diynone **6** was best performed in two steps to maximize 6-endotrig cyclization to give chalcogenopyranone products and to minimize 5-exotrig cyclization to form five-membered dihydrochalcogenophene products.[19] The controlled addition of ethanol to diynone **6** in a mixture of 0.25 M sodium ethoxide in ethanol/tetrahydrofuran gave an 81:19 mixture of enol ethers **9**. The addition of the disodium chalcogenides (from the corresponding element and sodium borohydride in sodium ethoxide/ethanol) to solutions of the enol ethers **9** gave the chalcogenopyranones **5** as the only product in 74−89% isolated yields.

The addition of the Grignard reagent prepared from 4-bromo-*N*,*N*-dimethylaniline to chalcogenopyranones **5** and dehydration of the intermediate alcohols with hexafluorophosphoric acid gave dyes **2**−**4** as the hexafluorophosphate salts.[19] The hexafluorophosphate anions were exchanged for chloride anions with an ion-exchange resin to give dyes **2**−**4**.

Absorption Spectra of Dyes 2−4. In other chalcogenopyrylium dye series, replacing a lighter chalcogen atom with a heavier atom leads to a bathochromic shift in the absorption maximum.[14a,16,19] The same trend was observed in dyes **2**−**4** as shown in Table 1. What is somewhat surprising in this series is the observation that the sequential change in heteroatom gives changes in absorption maxima similar in magnitude to those observed in the 2,6-diphenyl-4-(dimethylamino)phenylchalcogenopyrylium dyes **10** (Chart 1; λ_{max} of 593 nm for thiopyrylium dye **10a**, 630 nm for selenopyrylium dye **10b**, and 651 nm for telluropyrylium dye **10c**). The additional dialkylamino substituents in **2**−**4** should help delocalize the positive charge, and one might expect the contribution of the heteroatom in the chalcogenopyrylium ring to be diminished, especially since delocalization of the positive charge between the nitrogen atoms of the anilino groups at the 2- and 4-positions or the 2- and 6-positions produces cyanine chromophores of significant length. For dyes **2**−**4**, the absorption band is broadened with three (dimethylamino)phenyl substit-

Scheme 2[a]

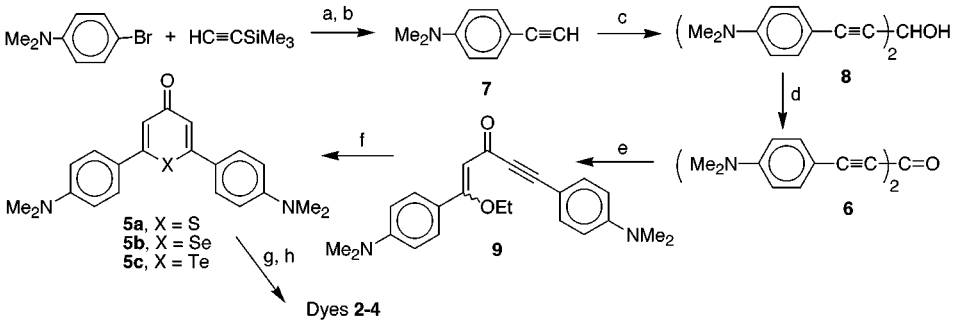

[a] Reagents: (a) $(PPh_3)_2PdCl_2$, PPh_3, CuI_2, piperidine (90%); (b) Bu_4NF (1.1 equiv), THF/H_2O (7:1) (82%); (c) 1.0 equiv *n*-BuLi, THF, then HCO_2Me (0.5 equiv) (57%); (d) MnO_2, CH_2Cl_2 (81%); (e) 0.25 M NaOEt in EtOH/THF; (f) S, Se, or Te, $NaBH_4$ (2.5 equiv), 0.1 M NaOEt in EtOH, add Na_2X to **9**; (g) (i) $Me_2NC_6H_4MgBr$, (ii) HPF_6; (h) Amberlite IRA-400 (Cl).

Table 1. Physical Properties of, Rates of Addition of Water/Hydroxide [k_1(obs)] to, Rates of Ring-Opening of Resulting Hemiketal [k_2(obs)] from, Reversibility of Water Addition (K_{eq}) to, and Initial Rates of Inhibition of Mitochondrial Cytochrome *c* Oxidase by Chalcogenopyrylium Dyes **2**−**4**

		hydrolysis						
dye	λ_{max} (log ϵ)[a]	k_1(obs), 10^{-4} s^{-1}	K_{eq}	k_2(obs), 10^{-5} s^{-1}	log *P*	$E°$(red),[b] V vs Fc/Fc^+	$\Phi(^1O_2)$[c]	% inhibn, J/cm^2 [d]
2	594 (4.76)	1.0 ± 0.1	0.16	2.2 ± 0.2	2.2	−0.62	0.020 ± 0.004	0.82
3	631 (4.76)	2.4 ± 0.3	0.17	1.7 ± 0.1	2.2	−0.70	0.064 ± 0.006	0.78
4	672 (4.74)	2.4 ± 0.3	0.30	1.1 ± 0.1	2.3	−0.76	0.037 ± 0.006	0.38

[a] In methanol. [b] 5×10^{-4} M solutions of **2**−**4** in CH_2Cl_2 with 0.2 M $Bu_4N^+BF_4^-$ as supporting electrolyte at a Pt disk electrode. Separation of E_c and E_a was <0.07 V at a scan rate of 0.05 V s^{-1}. [c] In methanol. [d] The inhibition values were established on the basis of constant absorbance (optical density of 0.20 ± 0.02 in a 1-cm quartz cuvette at maximum absorption in water) from sample to sample. Total light energy was measured over 530−750 nm assuming that each dye would absorb the same fraction of the total energy if absorbance of the samples was the same.

uents, perhaps due to contributions from all of the different length π-chromophores in the dye molecule. However, the maxima of absorption follow exactly the same trends as is observed in more simple chromophores.

Hydrolytic Stability. For the chalcogenopyrylium dyes **1** that have been evaluated as sensitizers for PDT,[14a,16] the major metabolic pathway observed for loss of dye is hydrolysis. The addition of water or hydroxide to the chromophore results in a loss of the long-wavelength absorption.[21,22] Hydrolytic stability impacts the circulating lifetime of the sensitizer in biological systems, the lifetime of the sensitizer at the active site, formulations for delivery of the sensitizer, and the distribution of metabolites from the sensitizer found in vivo. The circulating half-life of **1a**, which has photophysical properties that are optimal for PDT,[14a,16] is on the order of 20 min as determined with an in vivo spectrophotometer in BALB-c mice.[22] We measured the rates of hydrolysis for telluropyrylium dye **1a** as a control and for dyes **2**−**4** in RPMI-1640 growth medium at pH 7.4 with 5% added fetal calf serum to mimic conditions in vivo.

The initial step in the hydrolysis of chalcogenopyrylium salts involves the addition of hydroxide/water to the ring.[21] Addition can occur at the 2-, 4-, or 6-position of the ring, and the addition is reversible. Addition to the 4-position does not lead to an irreversible step. However, for the pyrylium ring (X = O), addition to the carbon at the 2-position (or C_6 in unsymmetrical pyrylium salts) generates a cyclic hemiacetal intermediate **11** that can rearrange to give a 2-pentene-1,5-dione **12** (Scheme 3). At higher pH, the addition of hydroxide and not water will dominate the kinetics of hydrolysis.[21b]

For the pyrylium ring, all of the steps of Scheme 3 are presumably reversible since acidification of the

Scheme 3

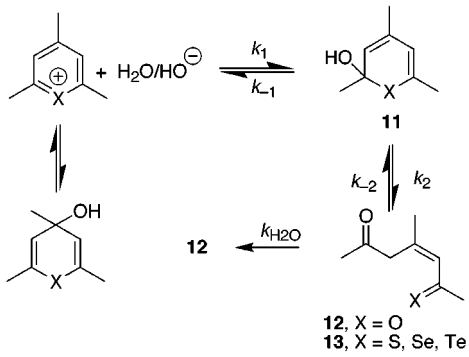

pentenedione **12** regenerates the pyrylium heterocycle.[21b] If the ring-opening step is fast (k_2) relative to the initial addition of hydroxide/water (k_1), then k_1 will be rate-determining and neither k_{-1} nor k_2 will be resolved. If the initial addition of hydroxide/water is fast relative to k_2, then the equilibrium between the cyclic hemiacetal and the pyrylium ring should be established (K_{eq}) followed by the slower ring-opening step (k_2). If k_1 and K_{eq} are large and the pH is high, the initial addition of hydroxide/water to the pyrylium ring may dominate the kinetics and k_2 will not be readily apparent even though it is rate-determining.

For dyes **2**−**4**, the 2-pentene-1,5-dione product will only be formed following hydrolysis of an intermediate thione, selenoketone, or telluroketone **13** from **2**−**4**, respectively. Consequently, the hydrolysis of dyes **2**−**4** is irreversible if ring-opening occurs.

At pH 7.4 in RPMI-1640 growth medium with 5% added fetal calf, the rate of hydrolysis as a function of time was fortuitously biphasic for dyes **1a** and **2**−**4**. An initial, rapid process [k_1(obs)] was followed by a second process [k_2(obs)] that was slower. Both processes fol-

lowed first-order kinetics. From these data, k_1(obs), K_{eq}(pH 7.4),[23] and k_2(obs) were measured, and their values are compiled in Table 1. It should be noted that at higher pH, k_1(obs) for hydrolysis is dominated by the $k_1[HO^-]$ term and k_2 is not observed, while at lower pH, the $k_1[HO^-]$ term is not observed as a discrete initial step. For dyes **2**−**4**, hydrolysis of the intermediate thione, selenoketone, or telluroketone could not be resolved suggesting that k_{H_2O} is fast relative to k_2(obs). For telluropyrylium dye **1a**, K_{eq}(pH 7.4) was 0.14 with a k_1(obs) of 5.8×10^{-4} s^{-1} at 37 °C. For this system, k_2(obs) was 7.3×10^{-5} s^{-1} and the half-life for this irreversible step is 160 min at 37 °C.

Dyes **2**−**4** were slower to hydrolyze than dye **1a** with half-lives of 525, 680, and 1050 min for **2**−**4**, respectively. Within the dye series **2**−**4**, k_1 and k_2 each varied by a factor of 2, which is indicative that the heteroatom has little effect on the rate of hydrolysis. However, dyes **2**−**4** are 3−7-fold more stable to hydrolysis than telluropyrylium dye **1a** and should have an appropriately longer circulating lifetime in vivo.

***n*-Octanol/Water Partition Coefficients as Markers for Lipophilicity.** The selective accumulation of Rh-123 in the mitochondria of neoplastic cells is thought to be responsible for the toxicity of Rh-123 toward cancer cells.[7] The selective accumulation appears to be a function of the net positive charge on Rh-123 and consequent affinity for the negative environment of the mitochondrial membrane. Although Rh-123 exists predominantly in ionic form in aqueous solution, it remains lipophilic enough to permeate the hydrophobic barrier of the plasma and mitochondrial membranes. The selective accumulation of AA1 in neoplastic cells[17] is believed to follow the model of Rh-123.

Telluropyrylium dye **1a**, Rh-123, and AA1 are all described as cationic, lipophilic dyes.[7,14a,15] The standard measure to predict lipophilicity is the *n*-octanol/water partition coefficient (*P*), which is expressed as a value of log *P*. In our hands, the value of log *P* for Rh-123 is 1.5 and the value of log *P* for AA1 is 1.9. The telluropyrylium dye **1a** has a slightly larger value of log *P* at 2.4.[14a] As shown in Table 1, the dyes **2**−**4** are more lipophilic than Rh-123 and AA1 and are only slightly less lipophilic than dye **1a**. Consequently, one might expect the dyes **2**−**4** to display similar mitochondrial accumulation as is observed with **1a**, Rh-123, and AA1.

Reduction Potentials of Dyes 2−4. One concern with respect to the use of mitochondrial-specific, cationic photosensitizers for PDT is the direct reduction of the sensitizer by the redox cascade in the mitochondria. While reduction of a cationic chemotherapeutic agent may lead to inhibition of mitochondrial function and cell death, reduction of a photosensitizer bleaches the chromophore and renders the material useless as a photosensitizer.

The reduction potentials of dyes **2**−**4** were determined by cyclic voltammetry, and values of $E°$ for the cation/neutral radical couple are compiled in Table 1. As is observed with other chalcogenopyrylium dyes, replacing a heavier chalcogen atom with a lighter chalcogen atom in the ring leads to a cathodic (negative) shift in reduction potential. All three of the dyes **2**−**4** have reduction potentials more negative than dye **1a** ($E°$ of −0.42 V), which survives the mitochondrial environment to function as a photosensitizer.[14a] Similarly, dyes **2**−**4** should not be reduced in the mitochondria and should function as photosensitizers if localized there.[14a]

Quantum Yields for Singlet Oxygen for Dyes 2−4. Many of the cationic photosensitizers such as the Victoria blues,[9] methylene blues[10] and the related nile blues,[11] cyanine dyes,[12] rhodacyanine dyes,[13] and telluropyrylium dyes **1a** and **1b**[14] generate singlet oxygen upon irradiation in aerated solvents. The singlet oxygen produced is thought to be responsible for part, if not all, of the biological damage that is observed from PDT with these sensitizers. The thiopyrylium dye AA1 is similar in structure to the cationic sensitizers described above but is described as having no phototoxicity, which suggests a low quantum yield for singlet oxygen generation.[15] Chalcogenopyrylium dyes **2**−**4** are structurally related to AA1, but the two amino groups of AA1 have been replaced with dimethylamino groups. All three dyes **2**−**4** were found to generate singlet oxygen upon irradiation and their singlet oxygen quantum yields [$\Phi(^1O_2)$] are compiled in Table 1.

The incorporation of the heavy atoms selenium and tellurium had distinctly different effects in the photosensitizer classes represented by dyes **1** and dyes **2**−**4**. In the chalcogenopyrylium dye series **1**, values of $\Phi(^1O_2)$ reflect the importance of spin−orbit effects on the rate of intersystem crossing from the singlet excited state to the triplet excited state.[16] Spin−orbit effects change as a function of Z^4, where Z is the atomic number of the heavy atom in the molecule. Replacing a sulfur atom in **1c** [$\Phi(^1O_2) = 0.0006$] with a selenium atom in **1d** [$\Phi(^1O_2) = 0.007$] gave an approximate 10-fold increase in $\Phi(^1O_2)$, while replacing the sulfur atom with a tellurium atom in **1e** [$\Phi(^1O_2) = 0.07$] gave an approximate 100-fold increase in singlet oxygen quantum yield as expected from spin−orbit effects.[14a,16]

While spin−orbit effects are manifest in the particular π-framework of chalcogenopyrylium dyes **1**, no such trend is observed with chalcogenopyrylium dyes **2**−**4** where values of $\Phi(^1O_2)$ vary by little more than a factor of 3. Furthermore, the value of $\Phi(^1O_2)$ for selenopyrylium dye **3** is largest in the series. Clearly, factors other than spin−orbit effects from the presence of the heavier chalcogens selenium and tellurium also influence the quantum yields of singlet oxygen generation in dyes **2**−**4**.

The value of $\Phi(^1O_2)$ of 0.020 for thiopyrylium dye **2** is more than 30-fold larger than the value of $\Phi(^1O_2)$ of 0.0006 measured for **1c**. Since no heavy atoms are present, the cyanine-like carbon π-framework **I** (Chart 2) must be important to the generation of singlet oxygen. The substitution of the heavier chalcogen atoms selenium and tellurium onto the π-framework should promote intersystem crossing. However, the substitution also distorts the carbon π-framework as shown in **II** and **III** (Chart 2). In the pyrylium ring (**II**), the C−O bond length is 1.37 Å, while the C−O−C bond angle and the angles *a*, *b*, and *c* marked in **II** are all approximately 120°.[24] The geometry of the central chalcogenopyrylium ring changes significantly as one goes down the periodic table. The selenopyrylium ring (**III**, X = Se) has a C−Se bond length of 1.89 Å, the C−Se−C bond angle is 99°, and the angles *a*, *b*, and *c* are 123°, 128°, and 120°, respectively.[24] The telluropyrylium ring (**III**, X = Te) is

Chart 2

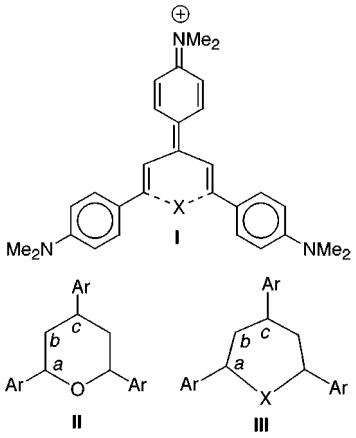

further distorted with a C−Te bond length of 2.07 Å, a C−Te−C bond angle of 94°, and the angles *a*, *b*, and *c* of 122°, 130°, and 122°, respectively.[26] The distortion in planarity of the chalcogenopyrylium ring also increases as one goes down the periodic table. While the pyrylium ring is nearly planar, the telluropyrylium ring is puckered in a boat shape with an approximately 8° dihedral angle down the central axis.[24] Consequently, increases in $\Phi(^1O_2)$ from spin−orbit effects may be offset by decreases in $\Phi(^1O_2)$ from distortion of the π-framework. In the dye series **2**−**4**, selenopyrylium dye **3** has the highest value of $\Phi(^1O_2)$ and may represent the best compromise between the benefits of spin−orbit effects and the twisting of the π-framework from geometric effects.

Although values of $\Phi(^1O_2)$ are small for dyes **2**−**4** relative to solution values of $\Phi(^1O_2)$ for other photosensitizers for PDT, the effects of rigidization in biological membranes on values of $\Phi(^1O_2)$ have not been determined. In other systems, such effects have been pronounced.[25] Rotational degrees of freedom in rigid, planar molecules such as the porphyrins, methylene blues, and nile blues are few, and the photophysics of these sensitizers will be little affected when the sensitizers reside in the biological membranes. In dyes **2**−**4**, rotation of the aryl groups in the excited state can release energy and return the dye to the ground state. If the dye were to reside in a biological membrane, rotational degrees of freedom might be reduced and effective values of $\Phi(^1O_2)$ might be much higher as has been observed in other systems.[25] In fact, dyes **1d** and **1f** with solution values of $\Phi(^1O_2) < 0.01$ have performed as efficient photosensitizers in vitro.[11a,16a] Since dyes **2**−**4** all have values of $\Phi(^1O_2) = 0.02$ and, consequently, should be better than **1d** and **1f** as sensitizers for PDT, all three dyes were evaluated in vitro as sensitizers for PDT.

Biochemistry

Inhibition of Cytochrome *c* Oxidase in Isolated Mitochondrial Suspensions. Chalcogenopyrylium dyes **2**−**4** are similar in structure to AA1 and Rh-123, which have been demonstrated to localize in the mitochondria of transformed cells.[7,15] Dyes **2**−**4** were evaluated as photosensitizers in vitro by measuring their effects on cytochrome *c* oxidase activity in isolated tumor mitochondria. Mitochondria, isolated from R3230AC rat mammary adenocarcinoma, were treated with 10^{-5} M

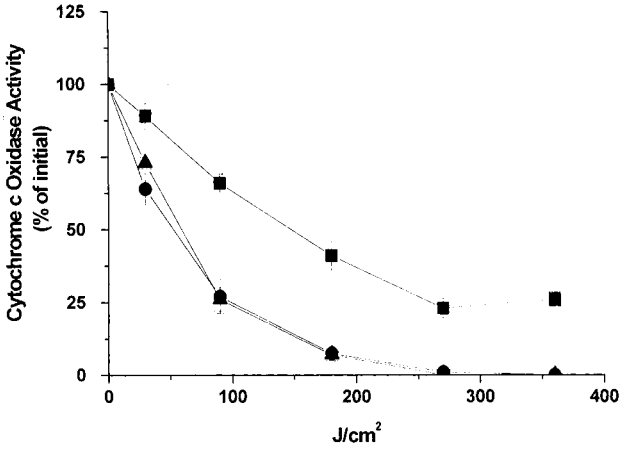

Figure 1. Effect of chalcogenopyrylium dye photosensitization on cytochrome *c* oxidase activity measured in isolated R3230AC tumor mitochondria. Details of experimental conditions are presented in the Experimental Section. Data are expressed as the percent of initial, preirradiation, cytochrome *c* oxidase activity in mitochondrial suspensions irradiated in the presence of 10 μM dye **2** (▲), dye **3** (●), or dye **4** (■). Each datum point represents the mean of at least three separate experiments performed in duplicate; bars are the SEM.

solutions of **2**−**4** for 5 min and centrifuged, and the pellet was resuspended. The cytochrome *c* oxidase activity in dye-treated mitochondrial suspensions was determined at selected times during 1 h of irradiation (Figure 1). Initial rates of inhibition over the first 10 min of exposure are compiled in Table 1. It should be noted that cytochrome *c* oxidase activity in dye-treated mitochondrial suspensions was not significantly altered during a 1-h incubation in the dark.

Cytochrome *c* oxidase, an inner mitochondrial membrane enzyme, is the last enzyme in the mitochondrial respiration chain.[26] Inhibition of cytochrome *c* oxidase during irradiation in the presence of a sensitizer may be due either to direct damage to the enzyme or to effects at a site(s) preceding it in the respiratory chain. Photosensitized inhibition could involve photoinduced single-electron transfer (SET) to oxygen resulting in the formation of either superoxide or another radical species or SET involving the ground state of the sensitizer. Alternatively, inhibition of cytochrome *c* oxidase could be a function of singlet-oxygen-induced damage from photochemical generation of singlet oxygen.

The observation that dye-treated mitochondria kept in the dark showed no inhibition of cytochrome *c* oxidase activity suggests that ground-state SET with the dye is not involved in the inhibition of the enzyme. This is also consistent with the large, negative values of $E°$ measured for the reduction potentials of dyes **2**−**4** (Table 1).

The photosensitized inhibition of mitochondrial cytochrome *c* oxidase by dyes **2**−**4** can be prevented by reducing the oxygen in the mitochondrial suspensions via nitrogen purging or by adding a singlet oxygen acceptor as illustrated in Figure 2 for dye **2**. Reduction of the oxygen concentration to 0 ± 2% prior to and during irradiation of the dye-treated mitochondria completely prevented the photosensitized inhibition of cytochrome *c* oxidase activity by each of the three dyes **2**−**4**. This observation strongly suggests that oxygen is involved in the inhibition process. The addition of the

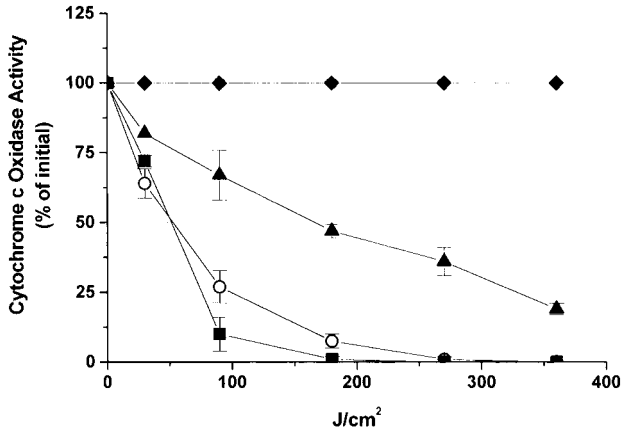

Figure 2. Effect of dye **2** (10 μM) photosensitization on mitochondrial cytochrome *c* oxidase activity in the presence of 0.080 M imidazole (▲), in the presence of 30 U of superoxide dismutase (■), in a nitrogen-purged/oxygen-reduced atmosphere (◆), or as an experimental control exposed to 10 μM dye **2** and light alone (○). Details of experimental conditions are described in the Experimental Section. Data are expressed as the percent of initial, preirradiation, cytochrome *c* oxidase activity in mitochondrial suspensions. Each datum point represents the mean of at least three separate experiments performed in duplicate; bars are the SEM.

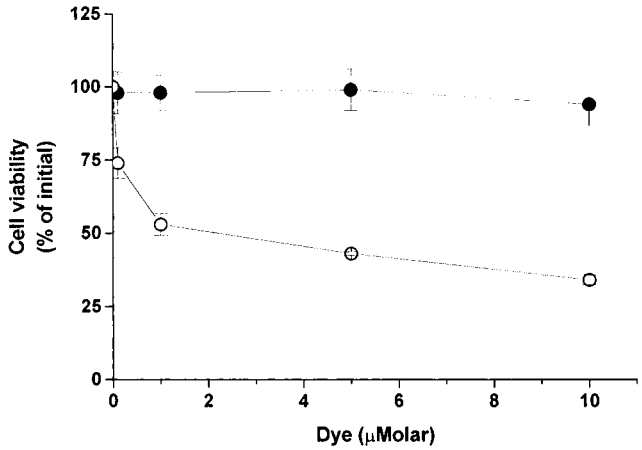

Figure 3. Effect of dye photosensitization on the cell viability of cultured R3230AC tumor cells. Details of experimental conditions are described in the Experimental Section. Data are expressed as percent viable cells, compared to untreated cells, for cells treated with dye **2** in the dark (■) or for cells treated with dye and 7.5 J cm^{-2} irradiation (□). Each datum point represents the mean percent viable cells calculated from at least three separate experiments performed in duplicate; bars are the SEM.

singlet oxygen acceptor imidazole[14a] at a concentration of 0.08 M to the dye-treated mitochondria prior to irradiation also prevented the inhibition of cytochrome *c* oxidase, although not to the same extent as conducting the studies in a reduced-oxygen, nitrogen-purged environment.

Superoxide dismutase (SOD), added at a concentration of 30 enzyme units/mL, did not reduce the photosensitized inhibition of cytochrome *c* oxidase observed with dyes **2**−**4** (Figure 2 for dye **2**). Since the addition of SOD did not decrease the level of photosensitized enzyme inhibition observed, excited-state SET from the dye to oxygen producing superoxide might be excluded as the major path for enzyme inhibition.

The data suggest that chalcogenopyrylium dyes **2**−**4** function as photosensitizers in isolated mitochondrial suspensions through singlet oxygen formation. Dyes **2**−**4** have values of $\Phi(^1O_2)$ in solution of 0.020−0.064 (Table 1). Rigidization of the dyes upon binding to the mitochondrial membrane may give much higher values of $\Phi(^1O_2)$ in vitro relative to the solution values.[25]

Effects of Dyes 2−4 on Cell Viability in Vitro. The dark and light-induced toxicities of dyes **2**−**4** were evaluated in cultures of R3230AC rat mammary adenocarcinoma cells. Cell cultures were incubated for 3 h in the dark with various concentrations of dyes **2**−**4** in minimum essential medium (α-MEM) at dye concentrations of 0.1, 1.0, 5.0, and 10 μM as illustrated in Figure 3 for dye **2**. Thiopyrylium dye **2** displayed the least dark toxicity of the three dyes and was essentially nontoxic at the concentrations employed. Selenopyrylium dye **3** and telluropyrylium dye **4** showed comparable dark toxicity with approximately 75% cell viability observed at 10 μM dye (Figures 4 and 5, respectively, in Supporting Information). Interestingly, thiopyrylium dye **2** is the least toxic dye in the dark and is also the most difficult to reduce (Table 1).

Exposure of cell cultures to 7.2 J cm^{-2} of 620-nm irradiation in the presence of dyes **2**−**4** resulted in reduced cell viability that was significantly greater ($P < 0.01$) than the toxicity observed for cells in the dark (Figures 3−5). The thiopyrylium dye **2** showed the highest potency. The phototoxicity for dyes **2**−**4** is not optimized. Photosensitizer-induced cytotoxicity at a given light dosage increased with dye concentration for all three dyes. However, thiopyrylium dye **2**, which displayed the least dark toxicity, appeared to be more effective than either selenopyrylium dye **3** ($P < 0.001$) or telluropyrylium dye **4** ($P < 0.05$).

Initial Toxicity Studies. In applications of PDT, the therapeutic dose of sensitizer for rodents is approximately 1−5 mg/kg.[1a,5] Female Fischer rats bearing implanted R3230AC tumors were given dyes **2**−**4** via tail-vein injection at a dosage of 10 mg/kg, which corresponds to 20 μmol/kg thiopyrylium dye **2**, 19 μmol/kg selenopyrylium dye **3**, and 17 μmol/kg telluropyrylium dye **4**. No morbidity or mortality was evident in animals observed for 24 h after injection of any of the three dyes, nor was tissue toxicity detectable upon gross examination of animals after sacrifice.

Summary and Conclusions

The chalcogenopyrylium dyes **2**−**4** represent a new class of photosensitizer for use in PDT. The dyes are similar in structure to AA1, which has shown antitumor activity in the dark with no enhancement by added light. All three dyes **2**−**4** display phototoxicity against R3230AC rat mammary adenocarcinoma cells in culture. Photosensitization of mitochondrial cytochrome *c* oxidase implicates singlet oxygen as a major contributor to the inhibition of this enzyme. Initial acute toxicity studies suggest that none of the three dyes are toxic at a likely therapeutic PDT dose. We are currently investigating the use of dyes **2**−**4** as sensitizers for PDT in vivo.

Experimental Section

General Methods. Solvents and reagents were used as received from Sigma-Aldrich Chemical Co. (St. Louis, MO) unless otherwise noted. Cell culture media was purchased from

GIBCO (Grand Island, NY). Fetal bovine serum (FBS) was obtained from Atlanta Biologicals (Atlanta, GA). Concentration in vacuo was performed on a Büchi rotary evaporator. NMR spectra were recorded at 30.0 °C on Varian Gemini-300, Inova 400, or Inova 500 instruments with residual solvent signal as internal standard: $CDCl_3$ (δ 7.26 for proton, δ 77.0 for carbon). Infrared spectra were recorded on a Perkin-Elmer FT-IR instrument. UV−visible near-IR spectra were recorded on a Perkin-Elmer Lambda 12 spectrophotometer or on a Sequential DX17 MV stopped-flow spectrometer (Applied Photophysics, Leatherhead, U.K.). Both were equipped with a circulating constant-temperature bath for the sample chambers. Elemental analyses were conducted by Atlantic Microanalytical, Inc.

4-(Dimethylamino)phenylacetylene (7).[22] 4-Bromo-*N*,*N*-dimethylaniline (19.35 g, 0.0967 mol), trimethylsilylacetylene (19.9 g, 0.193 mol), CuI (0.202 g, 1.06 mmol), and PPh_3 (0.51 g, 1.93 mmol) were dissolved in piperidine (400 mL). Bis(triphenylphosphine)palladium(II) chloride (0.204 g, 0.290 mmol) was added and the resulting mixture was heated at reflux for 8 h. The reaction mixture was concentrated in vacuo and saturated $NaHCO_3$ (200 mL) was added. The product was extracted with hexane (3 × 100 mL). The combined hexane extracts were washed with water and brine, dried over $MgSO_4$, and concentrated. The 2-(4-(*N*,*N*-dimethylamino)phenyl)trimethylsilylethyne[22] was isolated via chromatography on silica gel eluting with hexanes to give 18.9 g (90%) of product as a yellow solid: mp 82−84 °C; ^{1}H NMR ($CDCl_3$) δ 7.34 (d, 2 H, J = 8 Hz), 6.60 (d, 2 H, J = 8 Hz), 2.97 (s, 6 H), 0.25 (s, 9 H); IR ($CDCl_3$) 2962, 2146 cm^{-1}.

2-(4-(*N*,*N*-Dimethylamino)phenyl)trimethylsilylethyne (47.8 g, 0.219 mol) was dissolved in a mixture of 100 mL of THF and 15 mL of H_2O. A 1.0 M solution of tetrabutylammonium fluoride in THF (226 mL, 0.226 mol) was added dropwise at 0 °C and the reaction was stirred for 1 h at 0 °C. The reaction mixture was concentrated and H_2O (200 mL) was added. The products were extracted with hexane (6 × 75 mL) and the combined extracts were dried over $MgSO_4$ and concentrated. The product was purified via chromatography on silica gel eluted with hexane to give 26.0 g (82%) of **7** as a yellow-orange solid: mp 33−35 °C; ^{1}H NMR ($CDCl_3$) δ 7.36 (d, 2 H, J = 8 Hz), 6.61 (d, 2 H, J = 8 Hz), 2.96 (s, 6 H), 2.91 (s, 1 H); ^{13}C NMR ($CDCl_3$) δ 150.5, 133.2, 111.8, 108.9, 84.9, 74.7, 40.1; IR (CCl_4) 3262, 2923, 2224 cm^{-1}. Anal. ($C_{10}H_{11}N$) C, H, N.

1,5-Di-4-(dimethylamino)phenyl-1,4-pentadiyn-3-ol (8). A 2.5 M solution of *n*-butyllithium in hexanes (28.4 mL, 0.071 mol) was added dropwise to a solution of acetylene **7** (10.3 g, 0.071 mol) in 300 mL of anhydrous THF at −78 °C. After addition was complete, the reaction was stirred for 20 min at −78 °C. Methyl formate (2.13 g, 0.0355 mol) in 5 mL of anhydrous THF was added dropwise at −78 °C and the reaction was then warmed to ambient temperature over a 20-min period. Saturated $NaHCO_3$ (40 mL) was slowly added followed by an additional 200 mL of H_2O. The product was extracted with CH_2Cl_2 (6 × 50 mL). The combined organic extracts were washed with brine, dried over $MgSO_4$, and concentrated. The crude product was recrystallized from hexanes to give 6.41 g (57%) of 1,5-di-4-(dimethylamino)-phenyl-1,4-pentadiyn-3-ol (**8**) as a tan solid: mp 126−128 °C; ^{1}H NMR ($CDCl_3$) δ 7.32 (AA′BB′, 4 H, J ("doublet") = 8 Hz), 6.61 (AA′BB′, 4 H, J ("doublet") = 8 Hz), 5.53 (s, 1 H), 2.95 (s, 12 H), 2.31 (s, 1 H); ^{13}C NMR ($CDCl_3$) δ 150.3, 133.0, 111.6, 108.8, 85.4, 84.4, 53.5, 40.1; IR (CCl_4) 3262, 2923, 2224 cm^{-1}; EIMS m/z 318 (M^+). Anal. ($C_{21}H_{22}N_2O$) C, H, N.

1,5-Di-4-(dimethylamino)phenyl-1,4-pentadiyn-3-one (6). Manganese dioxide (12.8 g, 0.147 mol) was added to a solution of **17** (11.8 g, 0.0368 mol) in 100 mL of anhydrous CH_2Cl_2. The resulting mixture was stirred at ambient temperature for 2 h at which point an additional 6.4 g (0.074 mol) of MnO_2 was added. The reaction mixture was stirred 72 h and then filtered through a pad of Celite. The filter cake was washed with CH_2Cl_2 (5 × 75 mL). The combined organic filtrates were concentrated. The residue was purified via chromatography on silica gel eluted with CH_2Cl_2 followed by recrystallization from ethyl acetate−hexanes to give 9.36 g (81%) of **6** as a red solid: mp 143−145 °C; ^{1}H NMR ($CDCl_3$) δ 7.54 (AA′BB′, 4 H, J ("doublet") = 8 Hz), 6.65 (AA′BB′, 4 H, J ("doublet") = 8 Hz), 3.03 (s, 12 H); ^{13}C NMR ($CDCl_3$) δ 156.4, 147.4, 130.9, 107.1, 100.9, 90.7, 86.7, 35.6; IR (KBr) 2904, 2145, 1598 cm^{-1}; (+) FABMS m/z 317 (MH^+). Anal. ($C_{21}H_{22}N_2O$) C, H, N.

Preparation of Enol Ethers 9. Diynone **6** (3.16 g, 10.0 mmol) was dissolved in 200 mL of THF and 200 mL of 0.25 M sodium ethoxide in ethanol. The resulting solution was allowed to stand at 50 °C and the disappearance of **6** was monitored by thin-layer chromatography on silica gel eluted with CH_2Cl_2. After 0.5 h at 50 °C, loss of **6** was complete and the reaction mixture was poured into 100 mL of H_2O. The products were extracted with CH_2Cl_2 (3 × 15 mL) and the combined organic extracts were washed with brine, dried over $MgSO_4$, and concentrated to give 3.26 g (90%) of a red oil. The ^{1}H NMR spectrum of the crude reaction mixture was indicative of an 81:19 mixture of two enol ethers **9**. For the major enol ether **9**: ^{1}H NMR ($CDCl_3$) δ 7.53 (AA′BB′, 2 H, J ("doublet") = 9 Hz), 6.97 (AA′BB′, 2 H, J ("doublet") = 9 Hz), 6.68 (AA′BB′, 2 H, J ("doublet") = 9 Hz), 6.45 (AA′BB′, 2 H, J ("doublet") = 9 Hz), 5.69 (s, 1 H), 4.05 (q, 2 H, J = 7 Hz), 2.97 (s, 6 H), 2.96 (s, 6 H), 1.43 (t, 3 H, J = 7 Hz). For the minor enol ether **9**: ^{1}H NMR ($CDCl_3$) δ 7.53 (AA′BB′, 4 H, J ("doublet") = 9 Hz), 6.66 (AA′BB′, 2 H, J ("doublet") = 9 Hz), 6.64 (AA′BB′, 2 H, J ("doublet") = 9 Hz), 6.02 (s, 1 H), 4.22 (q, 2 H, J = 7 Hz), 3.02 (s, 6 H), 3.00 (s, 6 H), 1.22 (t, 3 H, J = 7 Hz). For the mixture **9**: IR (NaCl) 2170, 1603 cm^{-1}; EIMS m/z 362.2019 (M^+, calcd for $C_{23}H_{26}N_2O_2$ 362.1994).

Addition of Enol Ethers 9 to Disodium Chalcogenides. Enol ethers **9** were prepared as described above from diynone **6** (1.00 g, 3.16 mmol). The disodium chalcogenides, prepared from 3.79 mg-at of S (0.121 g), Se (0.300 g), or Te (0.484 g) and 0.122 g (3.79 mmol) of $NaBH_4$ in 40 mL of degassed 0.25 M sodium ethoxide in ethanol under an argon atmosphere, were added to the 0.25 M sodium ethoxide in ethanol/THF solution of enol ethers **9**. The reaction mixture was stirred for 15 min at ambient temperature and then poured into 200 mL of H_2O. The products were extracted with CH_2Cl_2 (4 × 50 mL) and the combined organic extracts were washed with brine, dried over $MgSO_4$, and concentrated. The residue was purified by chromatography on silica gel eluted with 20% ethyl acetate−CH_2Cl_2 to give chalcogenopyranones **5**. For disodium sulfide addition: 0.818 g (74%) of **5a**. For disodium selenide addition: 1.12 g (89%) of **5b**. For disodium telluride addition: 1.07 g (76%) of **5c**.

***4H*-2,6-Di-4-(dimethylamino)phenylthiopyran-4-one (5a):** mp 205 °C dec; ^{1}H NMR ($CDCl_3$) δ 7.56 (AA′BB′, 4 H, J ("doublet") = 9 Hz), 7.11 (s, 2 H), 6.73 (AA′BB′, 4 H, J ("doublet") = 9 Hz), 3.02 (s, 12 H); ^{13}C NMR ($CDCl_3$) δ 178.6, 148.8, 147.5, 123.3, 119.1, 118.8, 107.6, 35.7; IR (KBr) 1607, 1583 cm^{-1}; λ_{max} (CH_2Cl_2) 383 nm [α (3.0 ± 0.2) × 10^4 M^{-1} cm^{-1}]; ESMS m/z 351 (MH^+). Anal. ($C_{21}H_{22}N_2OS$) C, H, N.

***4H*-2,6-Di-4-(dimethylamino)phenylselenopyran-4-one (5b):** mp 215 °C dec; ^{1}H NMR ($CDCl_3$) δ 7.53 (AA′BB′, 4 H, J ("doublet") = 9 Hz), 7.19 (s, 2 H), 6.75 (AA′BB′, 4 H, J ("doublet") = 9 Hz), 3.03 (s, 12 H); ^{13}C NMR ($CDCl_3$) δ 180.7, 150.9, 147.4, 123.3, 120.5, 120.3, 107.7, 35.7; IR (KBr) 1602, 1516 cm^{-1}; λ_{max} (CH_2Cl_2) 396 nm [α (3.1 ± 0.2) × 10^4 M^{-1} cm^{-1}]; ESMS m/z 399 (MH^+, ^{80}Se-isotope). Anal. ($C_{21}H_{22}N_2OSe$) C, H, N.

***4H*-2,6-Di-4-(dimethylamino)phenyltelluropyran-4-one (5c):** mp 260 °C dec; ^{1}H NMR (CD_2Cl_2) δ 7.46 (AA′BB′, 4 H, J ("doublet") = 8 Hz), 7.17 (s, 2 H), 6.74 (AA′BB′, 4 H, J ("doublet") = 8 Hz), 3.01 (s, 12 H); ^{13}C NMR (CD_2Cl_2) δ 189.9, 153.9, 149.3, 130.6, 129.8, 129.7, 114.1, 41.9; IR (KBr) 1604, 1595 cm^{-1}; λ_{max} (CH_2Cl_2) 411 nm [α (3.2 ± 0.2) × 10^4 M^{-1} cm^{-1}]; ESMS m/z 449 (MH^+, ^{130}Te-isotope). Anal. ($C_{21}H_{22}N_2OTe$) C, H, N.

2,4,6-Tri-4-(dimethylamino)phenylthiopyrylium Hexafluorophosphate. 4-Bromo-*N*,*N*-dimethylaniline (0.171 g, 0.856 mmol) and magnesium turnings (0.072 g, 3 mg-at) were refluxed in THF (10 mL) for 2 h under an argon atmosphere. Pyranone **5a** (0.150 g, 0.428 mmol) was dissolved in THF (10 mL) and the resulting solution was added dropwise to the

reaction mixture. The resulting mixture was heated at reflux for an additional hour. The reaction mixture was cooled to ambient temperature and concentrated. The residue was taken up in acetic acid (10 mL) and the resulting solution was added dropwise to cold 10% HPF_6. The solid that precipitated was collected by filtration. The solid was dissolved in acetone (15 mL) and H_2O (300 mL) was added. The solid was collected by filtration and was recrystallized from CH_3CN to give 0.10 g (40%) of dye **2** as the PF_6 salt: mp > 260 °C; ^{1}H NMR (CD_2Cl_2) [300 MHz] δ 8.16 (s, 2 H), 7.92 ("doublet" AA′BB′, 2 H, J = 8.7 Hz), 7.80 ("doublet", 4 H, J = 9.0 Hz), 6.85 (m, 4 H), 3.17 (s, 3 H), 3.14 (s, 6 H); λ_{max} (CH_2Cl_2) 594 nm [α (5.8 ± 0.2) × 10^4 M^{-1} cm^{-1}]. Anal. ($C_{29}H_{32}F_6N_3PS$) C, H, N.

2,4,6-Tri-4-(dimethylamino)phenylthiopyrylium Chloride (2). The PF_6 salt of **2** (0.12 g, 0.20 mmol) and 1.0 g of Amberlite IRA-400 (Cl) ion-exchange resin were stirred in 25 mL of methanol for 1 h. The ion-exchange resin was removed by filtration and the filter cake was washed with 5 mL of methanol. The process was repeated twice with additional 1.0-g aliquots of the ion-echange resin. The final filtrate was concentrated, the residue was dissolved in 2 mL of CH_3CN, and the resulting solution was diluted to 25 mL with ether. Chilling precipitated the dye, which was collected by filtration to give 0.088 g (90%) of **2** as dark blue crystals: mp > 260 °C; ^{1}H NMR (CD_2Cl_2) [300 MHz] δ 8.16 (s, 2 H), 7.92 ("doublet" AA′BB′, 2 H, J = 8.7 Hz), 7.80 ("doublet", 4 H, J = 9.0 Hz), 6.85 (m, 4 H), 3.17 (s, 3 H), 3.14 (s, 6 H); λ_{max} (CH_2Cl_2) 594 nm [α (5.8 ± 0.1) × 10^4 M^{-1} cm^{-1}]. Anal. ($C_{29}H_{32}N_3SCl$) C, H, N.

2,4,6-Tri-4-(dimethylamino)phenylselenopyrylium Chloride (3). Selenopyrylium dye **3** was prepared from 4-bromo-*N*,*N*-dimethylaniline (0.206 g, 1.13 mmol), magnesium turnings (0.037 g, 1.5 mg-at), and selenopyranone **5b** (0.150 g, 0.378 mmol) as described above for the preparation of **2**. Product yield was 0.19 g (79%) of dye **3** as the PF_6 salt: mp > 260 °C; ^{1}H NMR (CD_2Cl_2) [500 MHz] δ 8.08 (s, 2H), 7.89 ("doublet" AA′BB′, 2 H, J = 9.0 Hz), 7.71 ("doublet", 4 H, J = 9.0 Hz), 6.85 ("doublet" AA′BB′, 2 H, J = 9.0 Hz), 6.80 ("doublet" AA′BB′, 2 H, J = 9.0 Hz), 3.14 (s, 3H), 3.12 (s, 6H); ^{13}C NMR (CD_2Cl_2) [300 MHz] δ 167.3, 157.4, 154.1, 131.2, 129.3, 125.1, 122.9, 121.3, 113.0, 112.8, 40.3 (2 sets of peaks overlap); λ_{max} (CH_2Cl_2) 631 nm [α (5.8 ± 0.2) × 10^4 M^{-1} cm^{-1}]. Anal. ($C_{29}H_{32}F_6N_3PSe$) C, H, N.

The hexafluorophosphate salt of **3** (0.13 g, 0.20 mmol) and 1.0 g of Amberlite IRA-400 (Cl) ion-exchange resin gave 0.10 g (94%) of **3** as shiny black crystals: mp > 260 °C; ^{1}H NMR (CD_2Cl_2) [500 MHz] δ 8.08 (s, 2H), 7.89 ("doublet" AA′BB′, 2 H, J = 9.0 Hz), 7.71 ("doublet", 4 H, J = 9.0 Hz), 6.85 ("doublet" AA′BB′, 2 H, J = 9.0 Hz), 6.80 ("doublet" AA′BB′, 2 H, J = 9.0 Hz), 3.14 (s, 3H), 3.12 (s, 6H); λ_{max} (CH_2Cl_2) 631 nm [α (5.8 ± 0.1) × 10^4 M^{-1} cm^{-1}]. Anal. ($C_{29}H_{32}N_3SeCl$) C, H, N.

2,4,6-Tri-4-(dimethylamino)phenyltelluropyrylium Chloride (4). Telluropyrylium dye **4** was prepared from 4-bromo-*N*,*N*-dimethylaniline (0.179 g, 0.896 mmol), magnesium turnings (0.044 g, 1.8 mg-at), and telluropyranone **5c** (0.200 g, 0.448 mmol) as described above for the preparation of **2**. Product yield was 0.22 g (70%) of dye **4** as the PF_6 salt: mp > 260 °C; ^{1}H NMR (CD_2Cl_2) [300 MHz] δ 7.75 (s, 2 H), 7.66 ("doublet" AA′BB′, 2 H, J = 9.0 Hz), 7.39 ("doublet" AA′BB′, 4 H, J = 8.7 Hz), 6.70 ("doublet" AA′BB′, 2 H, J = 8.7 Hz), 6.61 ("doublet" AA′BB′, 4 H, J = 9.0 Hz), 3.04 (s, 6 H), 3.02 (s, 12 H); ^{13}C NMR (CD_2Cl_2) [300 MHz] δ 165.3, 155.6, 151.2, 150.7, 128.0, 126.7, 125.0, 124.7, 122.1, 110.1, 37.4 (2 sets of peaks overlap); λ_{max} (CH_2Cl_2) 672 nm [α (5.5 ± 0.2) × 10^4 M^{-1} cm^{-1}]. Anal. ($C_{29}H_{32}F_6N_3PTe$) C, H, N.

The PF_6 salt of **4** (0.20 g, 0.29 mmol) and 1.0 g of Amberlite IRA-400 (Cl) ion-exchange resin gave 0.16 g (95%) of **4** as shiny, dark green crystals: mp > 260 °C; ^{1}H NMR (CD_2Cl_2) [300 MHz] δ 7.75 (s, 2 H), 7.66 ("doublet" AA′BB′, 2 H, J = 9.0 Hz), 7.39 ("doublet" AA′BB′, 4 H, J = 8.7 Hz), 6.70 ("doublet" AA′BB′, 2 H, J = 8.7 Hz), 6.61 ("doublet" AA′BB′, 4 H, J = 9.0 Hz), 3.04 (s, 6 H), 3.02 (s, 12 H); λ_{max} (CH_2Cl_2) 672 nm [α (5.5 ± 0.1) × 10^4 M^{-1} cm^{-1}]. Anal. ($C_{29}H_{32}N_3TeCl$) C, H, N.

Quantum Yields for Singlet Oxygen Generation. The singlet oxygen acceptor 1,3-diphenylisobenzofuran (DPBF), HPLC-grade methanol, and certified rose bengal and methylene blue were used as received from Aldrich Chemical Co. Quantum yields for singlet oxygen generation in air-saturated methanol were determined by monitoring the dye-sensitized photooxidation of DPBF[27] in a stopped-flow spectrophotometer (Applied Photophysics, Ltd.; ×18). The output beam of a 150-W Xenon arc lamp was passed through a monochromator (0.30-mm slits) to separate the 410-nm radiation and to direct it to the mixing chamber (approximate volume of 100 μL) via a flexible optical fiber to provide the excitation for DPBF. The excitation beam entered the chamber through a port that provides a 2-mm path length. The fluorescence of DPBF was monitored at a 90° angle to the excitation beam via a PMT (Hamamatsu) close-coupled to the chamber assembly. The fluorescence was passed through a 460-nm interference filter (Oriel) placed in front of the PMT window. The photolysis radiation was supplied by a 100-W QTH lamp (Oriel). The output of the lamp was passed through 590-nm long-pass and 660-nm interference filters (both from Oriel) and focused onto an input window of a flexible optical fiber. The photolysis light via the fiber reached the mixing chamber by entering through the 10-mm path length port. The solution of the sensitizer and the solution of DPBF were prepared separately to prevent sample degradation and were injected into the mixing chamber that was kept at (25.0 ± 0.1) °C via a circulating water bath. The decay of fluorescence of DPBF was then observed on a 200- or 2000-s time scale.

The fluorescence decays were analyzed using the routines provided with the stopped-flow instrument software package by fitting them to a first-order exponential decay function with a floating endpoint. A total of three or more measurements were recorded for each sample and the results averaged to obtain a mean value for the decay rate.

On the basis of our earlier work,[16] methylene blue has a singlet oxygen quantum yield [$\Phi(^1O_2)$] of 0.50 in methanol, which is close to the quantum yield of 0.52 determined for methylene blue in both ethanol and water.[28] The quantum yield for singlet oxygen generation by dyes **2**−**4** may be calculated by comparing the rates of the decay for the dye of interest and methylene blue (MB) at the same DPBF concentration and optical density at 660 nm:

$$\Phi(^1O_2)(\text{dye}) = [\Phi_{ox,DPBF}(\text{dye}) \times \Phi(^1O_2)(\text{MB})]/\Phi_{ox,DPBF}(\text{MB})$$

The rate of disappearance of DPBF can be expressed as follows:

$$-\text{d[DPBF]/d}t = \{I_a \times \Phi(^1O_2) \times k_r[\text{DPBF}]\}/\{k_r[\text{DPBF}] + k_d\}$$

where k_r is the rate of reaction of DPBF, k_d is the rate of decay of singlet oxygen, and I_a is the absorbed light.[29] At low concentrations of DPBF, where k_r[DPBF] ≪ k_d[DPBF] < 3 μM, $k_d = 1.0 \times 10^{-5}$ s^{-1},[30] first-order decay kinetics were observed. The values of $\Phi(^1O_2)$ for the dyes **2**−**4** were corrected for triplet quenching by the previously described method.[30]

The value of $\Phi(^1O_2)$ for **2** was confirmed with rose bengal where $\Phi(^1O_2) = 0.76$.[31] Dye **2** gave $\Phi(^1O_2)$ of 0.020 ± 0.004 in comparisons to rose bengal, which is identical to the value obtained with methylene blue.

Electrochemical Procedures. A Princeton Applied Research model 173 potentiostat/galvanostat and a model 175 Universal Programmer were used for the electrochemical measurements. The working electrode for cyclic voltammetry was a platinum disk electrode (diameter, 1 mm) obtained from Princeton Applied Research. The auxiliary electrode was a platinum wire. The reference for cyclic voltammetry was the Fc/Fc^+ couple at +0.40 V at a scan rate of 0.1 V s^{-1}. All samples were run in J. T. Baker HPLC-grade dichloromethane that had been stored over 3A molecular sieves. Electrometric-grade tetrabutylammonium fluoroborate (Southwestern Analytical Chemicals, Inc.) was recrystallized from ethyl acetate−ether and then dried overnight at 80 °C before it was used as supporting electrolyte at 0.2 M. Argon was used for sample deaeration.

Hydrolysis Studies. Hydrolysis studies were conducted in RPMI-1640 growth medium at pH 7.4 with 5% added fetal calf serum. A 10-μL aliquot of a 0.03 M stock solution of dye in methanol was added to 3.0 mL of growth medium in a 1-cm^2 quartz cuvette and the rate of loss of dye was recorded spectrophotometrically in a thermostated cell at 37 ± 1 °C at λ_{max} for the dye. Values were measured in triplicate.

Determination of Partition Coefficients. The octanol/water partition coefficients were all measured at pH 7.4 in phosphate-buffered saline using UV−visible spectrophotometry. The measurements were done using a "shake flask" direct measurement.[32] Three to five minutes of mixing was followed by 1 h of settling time. Equilibration and measurements were made at 23 °C using a Perkin-Elmer Lambda 12 spectrophotometer. HPLC grade 1-octanol was obtained from Sigma-Aldrich.

Animals. All animals were cared for under the guidelines of the University Committee on Animal Resources at the University of Rochester.

Preparation of Mitochondrial Suspensions. The R3230AC mammary adenocarcinoma was transplanted subcutaneously in the axillary region of 80−100-g female Fischer 344 rats using the sterile trochar method.[33] Two to three weeks after transplantation when tumors had grown to 2−3 cm in diameter, the animals were sacrificed. The tumors were excised and placed in 0.9% sodium chloride on ice. The tissue was finely minced with scissors and homogenized on ice at a ratio of 1 g of tumor tissue to 5 mL of buffer containing 0.33 M sucrose, 1 mM dithiothreitol, 1 mM ethylene glycol bis(β-aminoethyl ether)-*N*,*N*,*N*′,*N*′-tetraacetic acid, 0.03% bovine serum albumin, and 0.1 M potassiom chloride (pH 7.4), using 30-s bursts with a Polytron PCU-2110 homogenizer at a setting of 6 (Brinkmann Ind., Westbury, NY). Preparation of isolated mitochondria from the homogenized tumor tissue followed a method described earlier.[34] Mitochondrial suspensions were divided into 0.5-mL aliquots (6−10 mg of mitochondrial protein/mL) and stored at −86 °C until used for in vitro experiments.

Exposure of Tumor Mitochondria to Dyes 2−4 in Vitro. Mitochondrial suspensions were removed from storage and thawed on ice. Dyes **2**−**4** were prepared by dissolving 2.5 mg of dye in 5.0 mL of 95% ethanol, which approximated a 1.0 mM solution for each of the three dyes studied. Final concentrations of the dyes were determined using their absorbance. Ten microliters of the dye/ethanol solution was transferred to 1.0 mL mitochondrial preparation buffer and the absorbance determined using a diode array spectrophotometer (HP8452A, Hewlett-Packard, Palo Alto, CA). The dyes in mitochondrial preparation buffer, at a final concentration that gave an OD of 0.2, were then added to mitochondrial suspensions (1.0 mL) and allowed to incubate in the dark on ice for 15 min. The dye/mitochondrial suspension was then centrifuged at 8000*g* for 3 min using an Eppendorf microcentrifuge (model 3200, Brinkmann Ind., Westbuty, NY), the supernatant was aspirated with a Pasteur pipet, and the pellet was resuspended in 1.0 mL of mitochondrial preparation buffer. The suspension was then transferred to a 3.0-mL quartz cuvette which was positioned in a focused, 1.0-cm diameter, filtered (530−750 nm) light beam emitted from a 750-W tungsten source. The intensity of the beam was uniform over the wavelength band used and adjusted to a fluence rate of 100 mW cm^{-2} using neutral density filters. Beam intensity was measured using a radiometer (model 210, Coherent Inc., Palo Alto, CA). The light was cooled by passing it through a water filter eliminating thermal effects as the sample temperature did not rise above 25 °C. The mitochondrial suspensions were magnetically stirred continuously during the irradiation period, 1.0 h. Aliquots, 10 μL, were removed at various times during irradiation for determination of cytochrome *c* oxidase activity. A portion of the mitochondria/dye suspension was maintained in the dark and determinations of cytochrome *c* oxidase activity were performed on aliquots from these samples as dark controls. Measurement of cytochrome *c* oxidase activity was performed according to a method described earlier.[34] Initial enzyme activity was adjusted to obtain a decrease in the reduced cytochrome *c* oxidase absorbance at 550 nm of 0.4−0.6 OD unit/min. Data are expressed as the percent of initial, preirradiation cytochrome *c* oxidase activity.

Exposure of Mitochondria to Dyes 2−4 and Oxygen Radical Quenchers or a Reduced Oxygen Environment. To determine whether singlet oxygen was the major factor involved in the inhibition of cytochrome *c* oxidase when tumor mitochondria were exposed to dyes **2**−**4** and light, we performed experiments using imidazole as a singlet oxygen quenching agent or superoxide dismutase to remove superoxide. Imidazole was added to mitochondria/dye suspensions at 80 mM prior to placement of the suspensions in the irradiation beam. Superoxide dismutase was added to mitochondria/dye suspensions at 30 enzyme units/mL. An oxygen-free environment was established by nitrogen purging of the sample in a specifically designed chamber described earlier.[35] Control samples containing dye but not exposed to light were maintained in the nitrogen-purged atmosphere in the dark for 1 h and no inhibition of mitochondrial cytochrome *c* oxidase activity was observed.

Cells and Culture Conditions. Cultured R3230AC rat mammary adenocarcinoma cells were used to study the dark and light toxicity of dyes **2**−**4**. Cells were cultured using single cell suspensions prepared from tumors using the method of Hissin and Hilf.[36] The cell line was maintained in passage culture on 100-mm diameter polystyrene dishes (Becton Dickinson, Franklin Lakes, NJ) with 10 mL of minimum essential medium (α-MEM) supplemented with 10% fetal bovine serum (FBS), 50 units mL^{-1} penicillin G, 50 μg mL^{-1} streptomycin, and 1.0 mg mL^{-1} fungizone (GIBCO, Grand Island, NY). Cultures were maintained at 37 °C in a 5% carbon dioxide humidified atmosphere (Forma Scientific, Marietta, OH). Cell counts were performed using a particle counter (model ZM, Coulter Electronics, Hialeah, FL).

Exposure of Cultured R3230AC Cells to Dyes 2−4 and Light. Cells were trypsinized from 100-mm dishes and counted, and 1.5 × 10^5 cells/mL of α-MEM plus 10% FBS were seeded per well on 12-well plates. Cells were incubated at 37 °C and allowed to reach 60−90% confluency, >3 × 10^5 cells/well. The medium was removed and α-MEM, without FBS or phenol red, containing 0, 0.1, 1.0, 5.0, and 10.0 μM dye **2**, **3**, or **4** was added. The concentration of the dye was determined by absorbance as described above for the mitochondrial experiments. Cells were incubated with the dye for 3 h in the dark at 37 °C, the medium was then removed, monolayers were washed once with sterile 0.9% NaCl, and 1.0 mL of α-MEM, minus FBS and phenol red, was added. Plates were then exposed to 620-nm laser light emitted from an argon-pumped dye laser (Inova 90, Coherent Inc., Palo Alto, CA) connected to a 400-μm fiber which was fitted with a GRIN lens (General Fiber Optics, Cedar Grove, NJ). This configuration allowed us to expand the light to provide uniform illumination over the whole 12-well plate. The selection of 620 nm was based on the equivalent optical density of the dyes measured in α-MEM. Dye absorbance at 10 μM was 0.18 for **2**, 0.25 for **3**, and 0.2 for **4** at 620 nm. The fluence rate of the emitted light, 8.0 mW cm^{-2}, was measured using a power meter (model 1815C, Coherent Inc., Palo Alto, CA). Each dish containing cells and the various concentrations of dyes **2**−**4** was exposed to light for 15 min for a total fluence of 7.2 J cm^{-2}. Concurrently, monolayers were exposed to the same conditions, media changes, and dye incubation but were maintained as dark controls. Cells that were exposed to laser irradiation but not to dyes **2**−**4** displayed no change in viability. Following irradiation, the medium was removed, fresh α-MEM containing 10% FBS and phenol red was added, and the cells were incubated in the dark for 24 h at 37 °C. Cells were then trypsinized and counted as described above. Data are expressed as percent viable cells, which compares cell numbers from treated monolayers with untreated control cells.

Statistical Analyses. All statistical analyses were performed using the Student's *t*-test for pairwise comparisons. A P value < 0.05 was considered significant.

Administration of Dyes 2−4. Stock solutions of dyes **2**−**4** at 5 mg of dye/mL in 1% ethanol/0.9% NaCl were prepared by first dissolving the dye in ethanol and diluting to the appropriate volume with 0.9% NaCl. When R3230AC tumors reached 0.50−0.60 cm in diameter (0.1−0.17 cm^3), usually 7−12 days after tumor implantation, the animals were given 200 μL of the dye solution (10 mg of dye/kg; 20 μmol/kg for dye **2**, 19 μmol/kg for dye **3**, 17 μmol/kg for dye **4**) via tail-vein injection.

Acknowledgment. The authors thank the National Institutes of Health (Grant CA69155 to M.R.D. and Grant CA36856 to R.H.) for support of this work.

Supporting Information Available: Figures 4 and 5 for dark and phototoxicity of dyes **3** and **4**, respectively. This material is available free of charge via the Internet at http://pubs.acs.org.

References

(1) (a) Dougherty, T. J.; Gomer, C. J.; Henderson, B. W.; Jori, G.; Kessel, D.; Korbelik, M.; Moan, J.; Peng, Q. Photodynamic Therapy. *J. Natl. Cancer Inst.* **1998**, *90*, 889−905. (b) Kato, H. Photodynamic Therapy for Lung Cancer − A Review of 19 Years' Experience. *J. Photochem. Photobiol. B: Biol.* **1998**, *42*, 96−99. (c) Guillemin, F.; Feintrenie, X.; Lignon, D. La Therapie Photodynamique du Cancer Bronchique. *Rev. Pneumol. Clin.* **1992**, *48*, 111−114. (d) Puolakkainen, P.; Schroder, T. Photodynamic Therapy of Gastrointestinal Tumors: A Review. *Digestive Diseases* **1992**, *10*, 53−60.

(2) Noske, D. P.; Wolbers, J. G.; Sterenborg, H. J. Photodynamic Therapy of Malignant Glioma. A Review of Literature. *Clin. Neurol. Neurosurg.* **1991**, *93*, 293−307.

(3) Moesta, K. T.; Schlag, P.; Douglass, H. O., Jr.; Mang, T. S. Evaluating the Role of Photodynamic Therapy in the Management of Pancreatic Cancer. *Lasers Surg. Med.* **1995**, *16*, 84−92.

(4) Sternberg, E. D.; Dolphin, D.; Brückner, C. Porphyrin-based Photosensitizers for Use in Photodynamic Therapy. *Tetrahedron* **1998**, *54*, 4151−4202.

(5) (a) Gomer, C. J. Preclinical Examination of First and Second Generation Photosensitizers Used in Photodynamic Therapy. *Photochem. Photobiol.* **1991**, *54*, 1093−1107. (b) Pass, H. I. Photodynamic Therapy in Oncology: Mechanisms and Clinical Use. *J. Natl. Cancer Inst.* **1993**, *85*, 443−456.

(6) (a) Wan, S.; Parrish, J. A.; Anderson, R. R.; Madden, M. Transmittance of Nonionizing Radiation in Human Tissue. *Photochem. Photobiol.* **1981**, *34*, 679−684. (b) Svaasand, L. O.; Ellingsen, R. Optical Penetration in Human Intracranial Tumors. *Photochem. Photobiol.* **1985**, *41*, 73−76.

(7) (a) Davis, S.; Weiss, M. J.; Wong, J. R.; Lampidis, T. J.; Chen, L. B. Mitochondrial and Plasma Membrane Potentials Cause Unusual Accumulation and Retention of Rhodamine 123 by Breast Adenocarcinoma-Derived MCF-7 Cells. *J. Biol. Chem.* **1985**, *260*, 13844−13850. (b) Lampidis, T. J.; Bernal, S. D.; Summerhayes, I. C.; Chen, L. B. Rhodamine-123 Is Selectively Toxic and Preferentially Retained in Carcinoma Cells in Vitro. *Ann. N. Y. Acad. Sci.* **1982**, *395*, 299−303. (c) Bernal, S. D.; Lampidis, T. J.; McIsaac, R. M.; Chen, L. B. Anticarcinoma Activity in vivo of Rhodamine 123, a Mitochondrial-Specific Dye. *Science* **1986**, *222*, 169−172.

(8) (a) Kessel, D.; Woodburn, K. Selective Photodynamic Inactivation of a Multidrug Transporter by a Cationic Photosensitizing Agent. *Br. J. Cancer* **1995**, *71*, 306−310. (b) Harapanhalli, R. S.; Roy, A. M.; Adelstein, S. J.; Kassis, A. I. [^{125}I/^{127}I/^{131}I]Iodorhodamine: Synthesis, Cellular Localization, and Biodistribution in Athymic Mice Bearing Human Tumor Xenografts and Comparison with [^{99m}Tc]Hexakis(2-methoxyisobutylisonitrile). *J. Med. Chem.* **1998**, *41*, 1, 2111−2117.

(9) (a) Modica-Napolitano, J. S.; Joyal, J. L.; Ara, G.; Oseroff, A. R.; Aprille, J. R. Mitochondrial Toxicity of Cationic Photosensitizers for Photochemotherapy. *Cancer Res.* **1990**, *50*, 7876−7881. (b) Morgan, J.; Whitaker, J. E.; Oseroff, A. R. GRP78 Induction by Calcium Ionophore Potentiates Photodynamic Therapy Using the Mitochondrial Targeting Dye Victoria Blue BO. *Photochem. Photobiol.* **1998**, *67*, 155−164.

(10) Noodt, B. B.; Rodal, G. H.; Wainwright, M.; Peng, Q.; Horobin, R.; Nesland, J. M.; Berg, K. Apoptosis Induction by Different Pathways with Methylene Blue Derivative and Light from Mitochondrial Sites in V79 Cells. *Int. J. Cancer* **1998**, *75*, 941−948.

(11) (a) Cincotta, L.; Foley, J. W.; Cincotta, A. H. Phototoxicity, Redox Behavior, and Pharmacokinetics of Benzophenoxazine Analogues in EMT-6 Murine Sarcoma Cells. *Cancer Res.* **1993**, *53*, 2571−2580. (b) Lin, C. W.; Shulok, J. R.; Kirley, S. D.; Bachelder, C. M.; Flotte, T. J.; Sherwood, M. E.; Cincotta, L.; Foley, J. W. Photodynamic Destruction of Lysosomes Mediated by Nile Blue Photosensitizers. *Photochem. Photobiol.* **1993**, *58*, 81−91. (c) Lin, C. W.; Shulok, J. R.; Kirley, S. D.; Cincotta, L.; Foley, J. W. Lysosomal Localization and Mechanism of Uptake of Nile Blue Photosensitizers in Tumor Cells. *Cancer Res.* **1991**, *51*, 2710−2719. (d) Cincotta, L.; Foley, J. W.; MacEachern, T.; Lampros, E.; Cincotta, A. H. Novel Photodynamic Effects of a Benzophenothiazine on Two Different Murine Sarcomas. *Cancer Res.* **1994**, *54*, 1249−1258.

(12) (a) Oseroff, A. R.; Ohuoha, D.; Ara, G.; McAuliffe, D.; Foley, J.; Cincotta, L. Intramitochondrial Dyes Allow Selective in vitro Photolysis of Carcinoma. *Proc. Natl. Acad. Sci. U.S.A.* **1986**, *83*, 9729−9733. (b) Ara, G.; Aprille, J. R.; Malis, C. D.; Kane, S. B.; Cincotta, L.; Foley, J.; Bonventre, J. V.; Oseroff, A. R. Mechanisms of Mitochondrial Photosensitization by the Cationic Dye, *N*,*N*′-Bis(2-ethyl-1,3-dioxylene)kryptocyanine (EDKC): Preferential Inactivation of Complex I in the Electron Transport Chain. *Cancer Res.* **1987**, *47*, 6580−6585. (c) Lee, C.; Wu, S. S.; Chen, L. B. Photosensitization by 3,3′-Dicyclohexyloxacarbocyanine Iodide: Specific Disruption of Microtubules and Inactivation of Organelle Motility. *Cancer Res.* **1995**, *55*, 2063−2069.

(13) (a) Modica-Napolitano, J. S.; Brunelli, B. T.; Koya, K.; Chen, L. B. Photoactivation Enhances the Mitochondrial Toxicity of the Cationic Rhodacyanine MKT-077. *Cancer Res.* **1998**, *58*, 71−75. (b) Modica-Nopolitano, J. S.; Koya, K.; Weisberg, E.; Brunelli, B. T.; Li, Y.; Chen, L. B. Selective Damage to Carcinoma Mitochondria by the Rhodacyanine MKT-077. *Cancer Res.* **1996**, *56*, 544−550. (c) Kawakami, M.; Koya, K.; Ukai, T.; Tatsuta, N.; Ikegawa, A.; Ogawa, K.; Shishido, T.; Chen, L. B. Synthesis and Evaluation of Novel Rhodacyanine Dyes That Exhibit Antitumor Activity. *J. Med. Chem.* **1997**, *40*, 3151−3160.

(14) (a) Detty, M. R.; Merkel, P. B.; Hilf, R.; Gibson, S. L.; Powers, S. K. Chalcogenapyrylium Dyes as Photochemotherapeutic Agents. 2. Tumor Uptake, Mitochondrial Targeting, and Singlet-Oxygen-Induced Inhibition of Cytochrome *c* Oxidase. *J. Med. Chem.* **1990**, *33*, 1108−1116. (b) Kessel, D. Intracellular Localization of a Chalcogenapyrylium Dye Probed by Spectroscopy and Sites of Photodamage. *Photochem. Photobiol.* **1991**, *53*, 73−78.

(15) Sun, X.; Wong, J. R.; Song, K.; Hu, J.; Garlid, K. D.; Chen, L. B. AA1, A Newly Synthesized Monovalent Lipophilic Cation, Expresses Potent in vivo Antitumor Activity. *Cancer Res.* **1994**, *54*, 1465−1471.

(16) Detty, M. R.; Merkel, P. B. Chalcogenapyrylium Dyes as Potential Photochemotherapeutic Agents. III. Solution Studies of Heavy Atom Effects on Triplet Yields, Quantum Efficiencies of Singlet Oxygen Generation, Rates of Reaction with Singlet Oxygen, and Emission Quantum Yields. *J. Am. Chem. Soc.* **1990**, *112*, 3845−3851.

(17) Detty, M. R.; O'Regan, M. B. *Tellurium-Containing Heterocycles*; The Chemistry of Heterocyclic Compounds Series; Taylor, E. C., Ed.; Wiley-Interscience: New York, 1994; Vol. 53, Chapter 3.

(18) (a) Detty, M. R.; Luss, H. R. Addition of Disodium Chalcogenides to 1,5-Bis(trimethylsilyl)penta-1,4-diyn-3-one. Syntheses, Structure, and Reactivity of the Parent α-*4H*-Chalcogenapyran-4-ones. *Organometallics* **1992**, *11*, 2157−2162. (b) Detty, M. R.; Hassett, J. W.; Murray, B. J.; Reynolds, G. A. α,4,4′-4-Chalcogenapyranyl-*4H*-chalcogenapyrans. Synthesis, Electrochemical Oxidation, and ESR Investigations of Radical-Cation States. *Tetrahedron* **1985**, *45*, 4853−4858.

(19) Detty, M. R.; Murray, B. J. Telluropyrylium Dyes. 1. 2,6-Diphenyltelluropyrylium Dyes. *J. Org. Chem.* **1982**, *47*, 5235−5242.

(20) Wong M. S.; Nicoud, J.-F. Synthesis and Computational Studies of Hyperpolarizable Zig-Zag Chromophores. *Tetrahedron Lett.* **1994**, *35*, 6113−6116.

(21) (a) Young, D. N.; Detty, M. R. Hydrolysis Studies of Chalcogenopyrylium Trimethine Dyes. I. Product Studies in Alkaline Solution (pH = 8) under Anaerobic and Aerobic Conditions. *J. Org. Chem.* **1997**, *62*, 4692−4700. (b) Young, D. N.; Serguievski, P.; Detty, M. R. Hydrolysis Studies of Chalcogenopyrylium Trimethine Dyes. 2. Chalcogen Atom Effects on the Rates of Hydrolysis of Chalcogenopyrylium Dyes. *J. Org. Chem.* **1998**, *63*, 5716−5721.

(22) Bellnier, D. A.; Young, D. N.; Detty, M. R.; Camacho, S.; Oseroff, A. R. pH-Dependent Chalcogenopyrylium Dyes as Potential Sensitizers for PDT. Selective Retention in Tumor by Exploiting pH Differences between Tumor and Normal Tissue. *Photochem. Photobiol.*, submitted for publication.

(23) In a buffered system, the concentration of hydroxide remains constant as does the concentration of water. We have chosen to express K_{eq}(pH 7.4) as a ratio of hydroxide addition product to chalcogenopyrylium dye.

(24) Wilkstrom, M.; Krab, K.; Saraste, M. *Cytochrome Oxidase-A Synthesis*; Academic: New York, 1981.

(25) Aveline, B. M.; Redmond, R. W. Can Cellular Phototoxicity Be Accurately Predicted on the Basis of Sensitizer Photophysics? *Photochem. Photobiol.* **1999**, *69*, 306−316.

(26) Reference 17, Chapter 4.
(27) Merkel, P. B.; Kearns, D. R. Comments Regarding the Rate Constant for the Reaction Between 1,3-Diphenylisobenzofuran and Singlet Oxygen. *J. Am. Chem. Soc.* **1975**, *97*, 462−463.
(28) Merkel, P. B.; Kearns, D. R. Radiationless Decay of Singlet Molecular Oxygen in Solution. An Experimental and Theoretical Study of Electronic-to-Vibrational Electron Transfer. *J. Am. Chem. Soc.* **1972**, *94*, 7244−7253.
(29) Wilkinson, F.; Helman, W. P.; Ross, A. B. Rate Constants for the Decay and Reactions of the Lowest Electronically Excited Singlet State of Molecular Oxygen in Solution. *J. Phys. Chem. Ref. Data* **1995**, *24*, 663−1021.
(30) Serguievski, P.; Detty, M. R. Electronic Substituent Effects in Quenching of $^1O_2$ by Diaryl Tellurides. *Organometallics* **1997**, *16*, 4386−4391.
(31) Gardin, E.; Lion, Y.; Van de Vorst, A. Quantum Yield of Singlet Oxygen Production by Xanthene Derivatives. *Photochem. Photobiol.* **1983**, *37*, 271−278.
(32) Sangster, J. In *Octanol−Water Partition Coefficients: Fundamentals and Physical Chemistry*; Wiley Series in Solution Chemistry; Fogg, P. G. T., Ed.; John Wiley and Sons: New York, 1997.
(33) Hilf, R.; Michel, I.; Bell, C.; Freeman, J. J.; Borman, A. Biochemical and Morphological Properties of a New Lactating Tumor Line in the Rat. *Cancer Res.* **1965**, *25*, 286−299.
(34) Gibson, S. L.; Hilf, R. Photosensitization of Mitochondrial Cytochrome C Oxidase by Hematoporphyrin Derivative and Related Porphyrins in Vitro and in Vivo. *Cancer Res.* **1983**, *43*, 4191−4197.
(35) Gibson, S. L.; Hilf, R. Interdependence of Energy Density, Drug Dose, and Oxygen on Hematoporphyrin Induced Photosensitization of Tumor Mitochondria. *Photochem. Photobiol.* **1985**, *42*, 367−373.
(36) Hissin, P. J.; Hilf, R. Effects of Insulinin Vivo and in Vitro on Amino Acid Transport into Cells from R3230AC Mammary Adenocarcinoma and Their Relationship to Tumor Growth. *Cancer Res.* **1978**, *38*, 3646−3651.

JM990134R